NEOPLASIA
www.neoplasia.com
Volume 24 Number xxx Month 2022 pp. 145–154

The renal clear cell carcinoma immune landscape

Omar A. Saad[a,1]; Wei Tse Li[a,1]; Aswini R. Krishnan[a,1]; Griffith C. Nguyen[a]; Jay P. Lopez[b]; Rana R. McKay[c]; Jessica Wang-Rodriguez[d]; Weg M. Ongkeko[a,*]

[a] Department of Surgery, University of California, San Diego, La Jolla, CA 92093, USA
[b] Division of Hematology and Oncology, New York-Presbyterian/Weill Cornell Medical College, NY, USA
[c] Department of Medicine, Division of Hematology/Oncology, University of California San Diego, San Diego, CA, USA
[d] Veterans Administration Medical Center and Department of Pathology, University of California, San Diego, La Jolla, California 92161, USA

Abstract

A comprehensive evaluation of the clear cell renal cell carcinoma (ccRCC) immune landscape was found using 584 RNA-sequencing datasets from The Cancer Genome Atlas (TCGA), we identified 17 key dysregulated immune-associated genes in ccRCC based on association with clinical variables and important immune pathways. Of the numerous findings from our analyses, we found that several of the 17 key dysregulated genes are heavily involved in interleukin and NF-kB signaling and that somatic copy number alteration (SCNA) hotspots may be causally associated with gene dysregulation. More importantly, we also found that key immune-associated genes and pathways are strongly upregulated in ccRCC. Our study may lend novel insights into the clinical implications of immune dysregulation in ccRCC and suggests potential immunotherapeutic targets for further evaluation.

Neoplasia (2022) 24, 145–154

Keywords: Renal clear cell carcinoma, TCGA

Introduction

Kidney cancers comprise a heterogeneous group of malignancies that affect nearly 270,000 patients [1]. Of the different types of kidney cancers, renal cell carcinomas (RCCs) originate within the renal cortex and account for 85% of all primary kidney neoplasms [2]. RCCs are divided into several histological subtypes, the most common of which is clear cell renal cell carcinoma (ccRCC, or KIRC), comprising 70-80% of RCCs [3]. The driving oncogenic event in ccRCC is attributed to VHL gene dysfunction resulting in accumulation of hypoxia-inducible factor (HIF), leading to downstream angiogenesis, cell growth, and cell proliferation [4]. Despite recent improvement in kidney cancer outcomes due to VEGF targeted therapies, kidney cancer still accounts for over 115,000 deaths annually worldwide and further progress is necessary to improve patient survival outcomes and for better patient selection for systemic therapy [1,5]. ccRCC is recognized as an immunogenic tumor due to its ability to induce adaptive immune responses, via recruitment of T-cells, and the presence of tumor-associated macrophages [6]. Several subsets of immune cells have been reported in ccRCC tumors, including 17 subtypes of tumor-associated macrophages and 22 subtypes of T-cells identified with mass spectrometry data and antibody panels [7]. Expression of immune checkpoint molecules on infiltrating T-cell surface correlates with ccRCC progression [8]. Immunotherapy has risen as a key therapeutic strategy in ccRCC treatment with the development of CTLA4-targeted therapies and PD-1/PD-L1 checkpoint inhibitors, such as the monoclonal antibody nivolumab [6]. PD-1 is often upregulated in ccRCCs, enabling ccRCC cells to avoid destruction by the immune system. By blocking PD-1, nivolumab has shown promise in increasing immune response against ccRCC cells but has often produced immune-related adverse events, including autoimmunity as well as milder side effects, including fatigue, skin rash, and nausea in some patients [9]. In addition, a large percentage of patients fails to respond successfully to PD-1 blockade, for reasons that remain largely unclear [10].

Several markers have been found that can partially predict response to PD-1 or PD-L1 blockade in ccRCC. PD-L1 has been shown as a marker for PD-L1 blockade response, but the correlation is controversial [11]. PD-1/PD-L1 blockade failure may be related to lack of angiogenesis,

* Corresponding author.
E-mail addresses: omar_saad@ucsb.edu (O.A. Saad), wtl008@ucsd.edu (W.T. Li), arkrishn@ucsd.edu (A.R. Krishnan), gcnguyen@ucsd.edu (G.C. Nguyen), rmckay@ucsd.edu (R.R. McKay), jessica.wang-rodriguez@va.gov (J. Wang-Rodriguez), wongkeko@ucsd.edu, rongkeko@health.ucsd.edu (W.M. Ongkeko).
[1] These authors contributed equally to this work.
Received 18 October 2021; accepted 20 December 2021

https://doi.org/10.1016/j.neo.2021.12.007

myeloid inflammation, and T-cell/IFN-γ activation, based on exploratory gene expression correlations [12]. On the genomics scale, loss-of-function mutations in *PBRM1* correlates with better response to PD-1/PD-L1 blockade in ccRCC [13].

It is necessary that we develop an in-depth understanding of the clinically relevant immune-associated landscape of ccRCCs in order to understand the causes of differential clinical effects of immunotherapy in ccRCC [14]. Therefore, in this study, we examined dysregulation of immune-associated (IA) genes in ccRCC and investigated their relevance to tumor formation. Using 512 RNA-sequencing datasets from The Cancer Genome Atlas (TCGA) of primary, untreated ccRCC tissues, we identified a panel of 17 key dysregulated IA genes in ccRCC from a total of 371 dysregulated and survival-associated IA transcripts. To gain insight into potential sources of IA gene dysregulation, we investigated the relationship among IA gene dysregulation, mutation, and copy number alteration occurrences in ccRCC to assess the ability of genomic alterations to modulate the ccRCC IA landscape. Mutations have been widely recognized as key driving events in malignant transformation, while SCNAs have been implicated in various cancer phenotypes due to rearrangement of large genomic regions [15,16]. With the recent recognition that microRNAs may function as key modulators of the tumor immune response, we explored the ability of these small transcripts to modulate IA gene. Finally, we performed gene set-level analyses by correlating expression of individual IA genes to expression of genes within cancer and immune-related signatures and pathways to gain a pathways-scale understanding of the immune-associated cancer development.

Results

Identification of dysregulated immune-associated (IA) genes in ccRCC

We performed differential expression analysis for TCGA ccRCC vs. adjacent normal samples and found 829 IA genes to be dysregulated between the cancer and normal cohorts (FDR<0.05, Table S1-S2). Since TCGA sequences the bulk tumor, mRNAs within all tumor-infiltrating immune cells would have been captured along with mRNAs within cancer cells. Therefore, IA genes we identified can be dysregulated in immune cell populations. After completing the workflow outlined in Fig. 1A, we identified 829 IA genes to be dysregulated in ccRCC and 371 of those to correlate with patient survival. We then proceed to identify a panel of 17 IA genes that we believe to be most critical to the biological phenotype of ccRCC immune landscape, based on clinical relevance and importance to immune processes (Table 1, Fig. 1B). Each of these metrics will be detailed in the sections below. 15 of the 17 genes are upregulated in ccRCC (Fig. 1C). These 17 genes are involved in a variety of immune processes, including interleukin, interferon, and NF-kB signaling as well as inflammation (Fig. 1D). A large fraction of the 17 genes, including *OSM, JAK3, IL20RB, NOD2, IFNG*, and *CEBPB*, are involved in interleukin signaling. A significant number of genes, including *HCST, NOD2, TNFSF13B, TNFSF14* are involved in NF-kB signaling.

Clinical significance of dysregulated IA genes in ccRCC

In order to evaluate the clinical relevance of IA genes in ccRCC, we examined their expression relative to clinical variables, including vital status, cancer status, pathologic stage, and histologic grade. The 17 IA genes may significantly modulate different clinical phenotypes (Kruskal-Wallis test, $p < 0.05$, Fig. 2A–E). 4 IA genes, *C1S, FCGR1A, JAK3*, and *PYCARD*, were found to display significantly elevated expression in TCGA patients whose tumors were not eliminated by the time of last follow-up (cancer status) (Fig. 2A). The dysregulation of 14 IA genes, all except *CMTM4, IL20RB*, and *OSM*, are strongly associated with worse pathologic N stage, or tumor invasion of nearby lymph nodes (Fig. 2B). 7 IA genes, *C1S, FCGR1A, IL20RB, JAK3, TNFSF13B, PYCARD*, and *NOD2*, are highly expressed in patients with metastasis (M1 stage) (Fig. 2C). Lastly, CD72 expression correlates with increasing pathologic stage, and C1S expression correlates with increasing histologic grade (Fig. 2D,E). Notably, *C1S, JAK3*, and *PYCARD*, all upregulated in ccRCC, are highly expressed in patients with tumors at last follow-up, in patients with higher pathological stage, and in patients with metastatic tumors. We also found that all 17 IA genes' expressions are significantly associated with overall survival in a manner consistent with the direction of their dysregulation in ccRCC (Cox regression, $p < 0.05$, Fig. 2F). Using just the 17 IA genes as a survival signature, we were able to predict ccRCC survival at 2,500 days with 79% accuracy (Fig. S1A). To ascertain that IA gene expressions' association with survival is not an effect of correlation between other clinical variables and survival, we performed a multivariate Cox regression analysis and found that the association between IA gene expression and survival is almost always stronger than the association between survival and clinical variables associated with IA genes (mostly pathologic N and M stages)(Table S3).

Table 1

Fold change and statistical significance of 17 key IA genes

Gene	Fold Change	Adjusted p-value
AIM2	8.25	5.75E-05
C1S	2.56	2.01E-07
CD72	6.59	6.45E-04
CEBPB	2.67	9.58E-06
CMTM4	0.27	9.28E-04
FCGR1A	8.53	8.70E-04
HCST	4.07	1.18E-06
IFNG	21.24	4.44E-03
IL20RB	15.31	3.35E-09
IRF6	0.33	3.65E-06
JAK3	5.44	5.48E-09
NOD2	5.46	1.54E-04
OSM	3.74	1.42E-03
PYCARD	4.22	5.03E-06
RNASE2	5.42	8.27E-05
TNFSF13B	5.69	1.03E-04
TNFSF14	13.8	4.53E-06

Association of IA gene dysregulation with genomic alterations in ccRCC

We used the REVEALER algorithm to explore the possible associations between genomic alterations and IA gene function. REVEALER generates a combination of likely causal genomic alteration events involved in modulating individual IA genes by exhaustively examining all alterations [17].

We found all 17 genes to have significant correlation with SCNAs (listed in Fig. 3A,B). We also observed that several SCNA hotspots, including deletions within chromosome arms 3p,14q, and 9p and amplifications within 20q, associate with the dysregulation of multiple IA genes (Fig. 3C). Interestingly, we did not find any mutations that correlated with the dysregulation of IA genes. None of the IA genes are associated with SCNAs on their own chromosomes, except for CEBPB, which is on 20q13 and correlated strongly with the amplification of 20q11. This result suggests that most IA genes are not dysregulated due to copy number changes on their own chromosomes.

To reveal the precise genes within SCNA loci that may alter the expression of IA genes, we correlated the expression of each IA gene to the expressions of all genes within each genomic locus associated with the IA gene (Spearman, $p < 0.05$). We observed that some genes, such as *PRKAR2A, HECTD1, ARHGAP5, ARHGEF12, FAM122A, SETD3, TXNDC16*, and

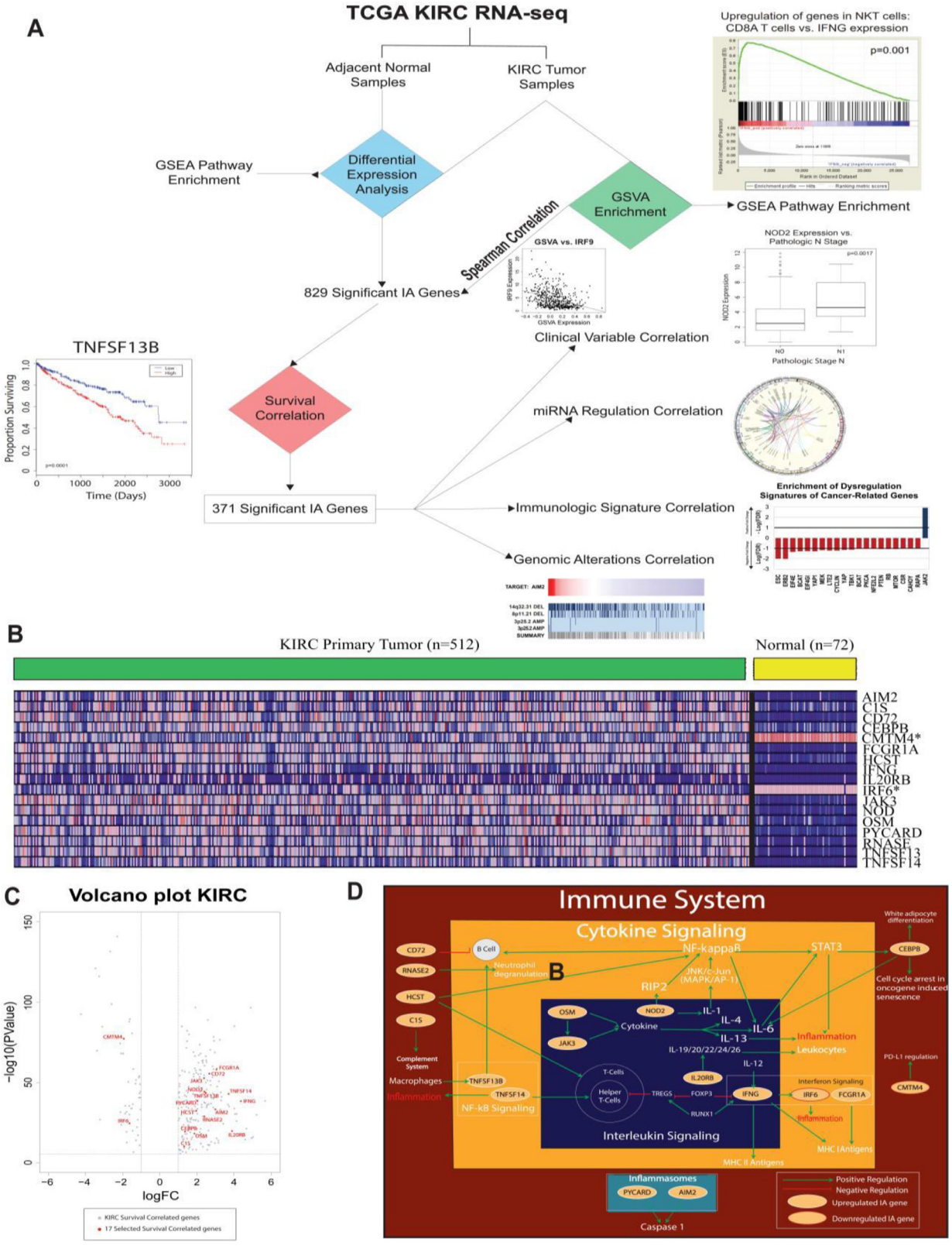

Fig. 1. Summary of study workflow and differential expression results. (**A**) Schematic of data processing procedures and algorithms utilized. (**B**) Heatmap of all IA genes differentially expressed when comparing ccRCC samples to normal samples. All genes correlate with patient survival (see Figure 2). In order from low to high expression, the heatmap displays dark blue, light blue, light red, and dark red. Asterisks next to gene names denote downregulated IA genes in ccRCC. (**C**) Volcano plot of differential expression significance vs. fold change in ccRCC samples vs. normal samples. All dots on the volcano plot represent survival-associated IA genes with significant fold change (|FC|<2) and corrected p-value ($p<0.05$). Selected 17 IA genes of interest in this study are labeled in red. (**D**) Schematic highlighting the interactions between selected IA genes of interest and key immune cells, processes, and pathways.

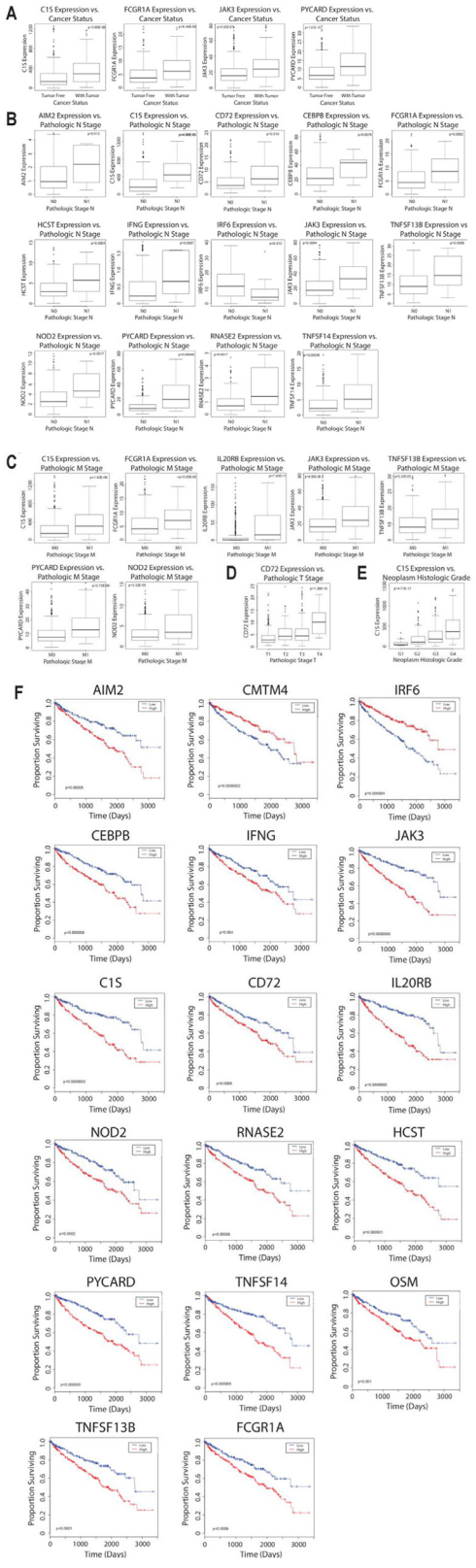

Fig. 2. Correlations of immune-associated gene expression with clinical variables and survival in ccRCC patients. Boxplots of IA gene expression vs. (**A**) cancer presence after treatment, (**B**) pathologic M stage, (**C**) pathologic N stage, (**D**) pathologic T stage, and (**E**) histologic grade (Kruskal-Wallis, $p<0.05$). (**F**) Kaplan-Meier survival plots for 17 selected IA genes (Cox regression, $p<0.05$).

BATF, exhibited much higher associations with the IA gene than other genes within the same region (Fig. 3D). Furthermore, many of the SCNA-related genes with high correlations are immune-related and may very likely affect the function of the IA gene (Fig. 3E,F). The 17 key IA genes are still the most clinically important IA genes, however, since only 69 out of 102 genes in SCNA loci that correlate with expression of a key IA gene also correlate with patient survival (Table S4). For the top 10 genes out of these 69 survival-associated genes, 7 out of 10 genes did not have a more significant correlation with survival than the survival correlation of key IA gene(s) they are associated with, suggesting that many of these genes may correlate with survival because their gene expression correlates with the expression of survival-associated IA genes (Table S5).

Identification of microRNAs involved in IA gene regulation

We selected miRNAs that are dysregulated in ccRCC and are predicted to target IA genes by the TargetScan software as candidate miRNAs that can potentially regulate IA genes (Table S6). Using gene set enrichment analysis (GSEA), we found the expressions of a large number of candidate miRNAs to be negatively enriched relative to IA gene expression for many of our IA genes ($p < 0.05$, Fig. 4A,B). Sample GSEA graphs indicate an inverse relationship between IA gene expression and expression of multiple miRNAs, as expected for miRNA-mediated gene silencing (Fig. 4C). Overall, this suggests a potential mechanism of IA gene regulation in ccRCC and also lends crucial insight into the potential use of miRNAs as therapeutic targets to modulate the immune response. We note that miRNAs do not serve as better ccRCC biomarkers than the 17 IA genes, as shown by their lower fold change in ccRCC samples, relative to the fold change of the 17 key IA genes (Table S7). We have also correlated the miRNA panel to patient survival and found that it is not as good a predictor of survival as the panel of 17 IA genes are (Fig. S1B).

Gene set-scale analysis of IA dysregulations in ccRCC

To further explore the impact of our 17 IA genes on the immune environment, we used GSEA to correlate expression of individual IA genes to expression of genes implicated in immunologic signature gene sets. We found *JAK3, IFNG*, and *TNFSF14* upregulation to associate more with NKT cell activity than conventional CD8+ T-cell activity (Fig. 5A–C). NKT cells are restricted to recognizing CD1d molecules, making them much less versatile than conventional CD8+ T-cells in recognizing tumor cells [18]. We found *JAK3* expression to associate with the expression profile of tumor-bearing monocyte cells, which may indicate *JAK3*'s potential ability to modulate monocyte phenotype in ccRCC (Fig. 5A). We also discovered that high *TNFSF14* expression correlated with high exhausted CD8+ T cell activity and inhibition of helper T cells generation, signifying *TNFSF14*'s potential role in diminishing adaptive immune function (Fig. 5B). Finally, we identified *OSM* to promote the resting state of T cells over the activated state, suggesting its potential role in immunosuppression as well (Fig. 5D).

We also explored cancer-related genes' dysregulation signatures and canonical cellular pathways implicated in ccRCC. We found that the downregulation of *MEL18, BMI1, STK33*, and *SNF5* and upregulation of *LEF1, KRAS*, and *IL2* are significantly correlated with ccRCC samples over normal samples (Fig. 5E). The downregulation of certain oncogenic signatures, such as for *BMI1* and *STK33* activity, in ccRCC suggests that anti-cancer mechanisms may still be present in ccRCC cells. GSEA analysis of canonical pathways dysregulated in ccRCC confirmed a general upregulation of immune processes in ccRCC, corroborating the immune upregulation indicated by the dysregulation of the 17 key IA genes (Fig. 5F). The only immunosuppressive IA pathway upregulated in ccRCC is the CTLA4 pathway. The majority of pathways downregulated in ccRCC are related to

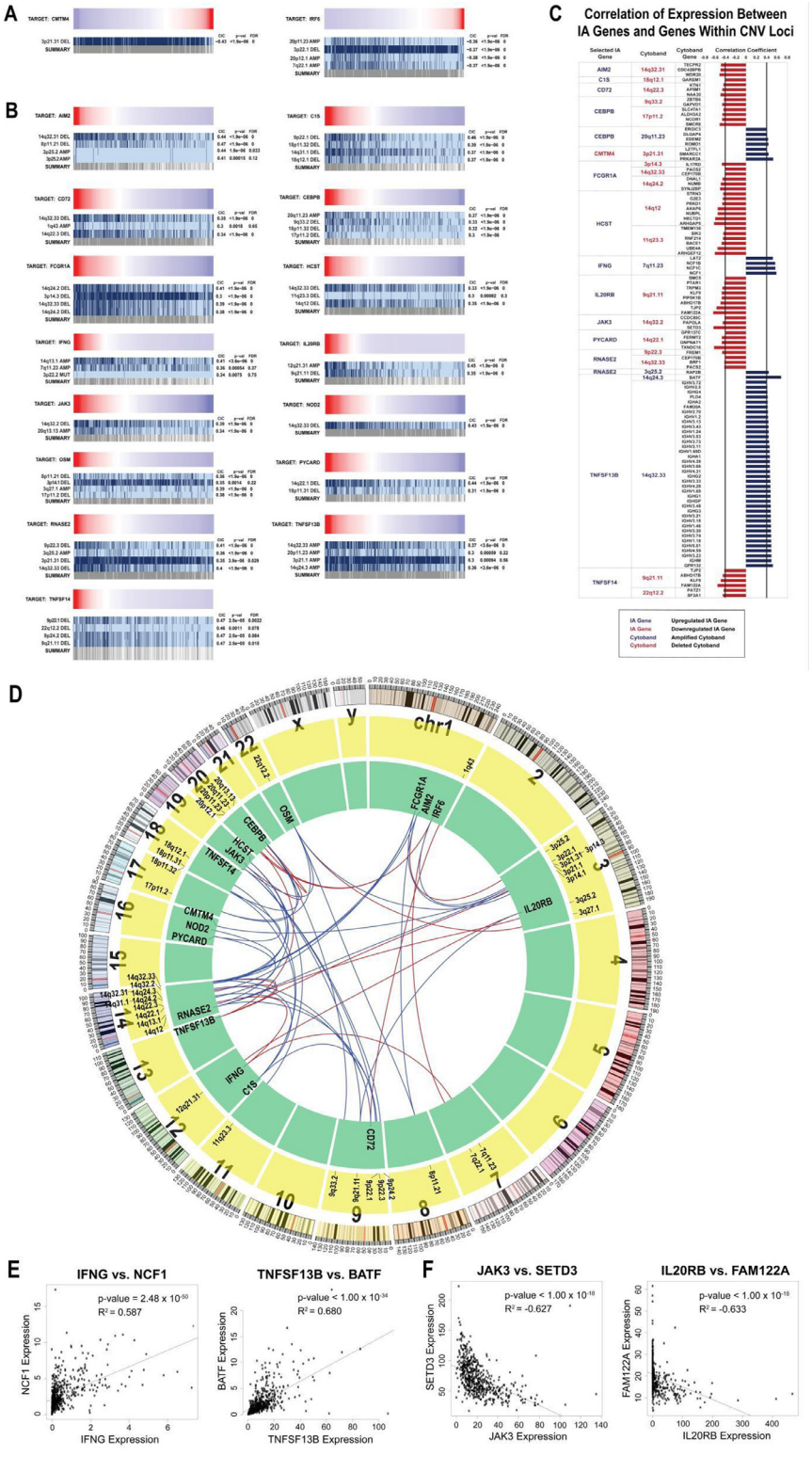

Fig. 3. Genomic alterations most associated with dysregulation of each IA gene. REVEALER plots of amplifications, deletions, or mutations that have the highest correlation with gene expression for (**A**) IA genes upregulated in ccRCC and (**B**) IA genes downregulated in ccRCC, with the significance threshold at |CIC| > 0.3. (**C**) Bar graphs of Spearman correlation coefficient of IA gene expression with expression of genes within SCNA regions seen in panels (A) and (B). Only correlations with correlation coefficient > 0.4 or <-0.4 are presented. (**D**) Circos plot visualizing chromosomal locations of correlations presented in panels (A) and (B). IA gene names are listed on the green circle, while SCNA regions are listed on the yellow circle. Blue lines connecting IA gene names to SCNA region names indicate that deletion of the regions correlate with dysregulation of the IA gene, while red lines indicate that amplification of the regions correlate with IA gene dysregulation. (**E**) Scatter plots of most significant direct (positive) correlations from panel (C). (**F**) Scatter plots of most significant inverse (negative) correlations from panel (C).

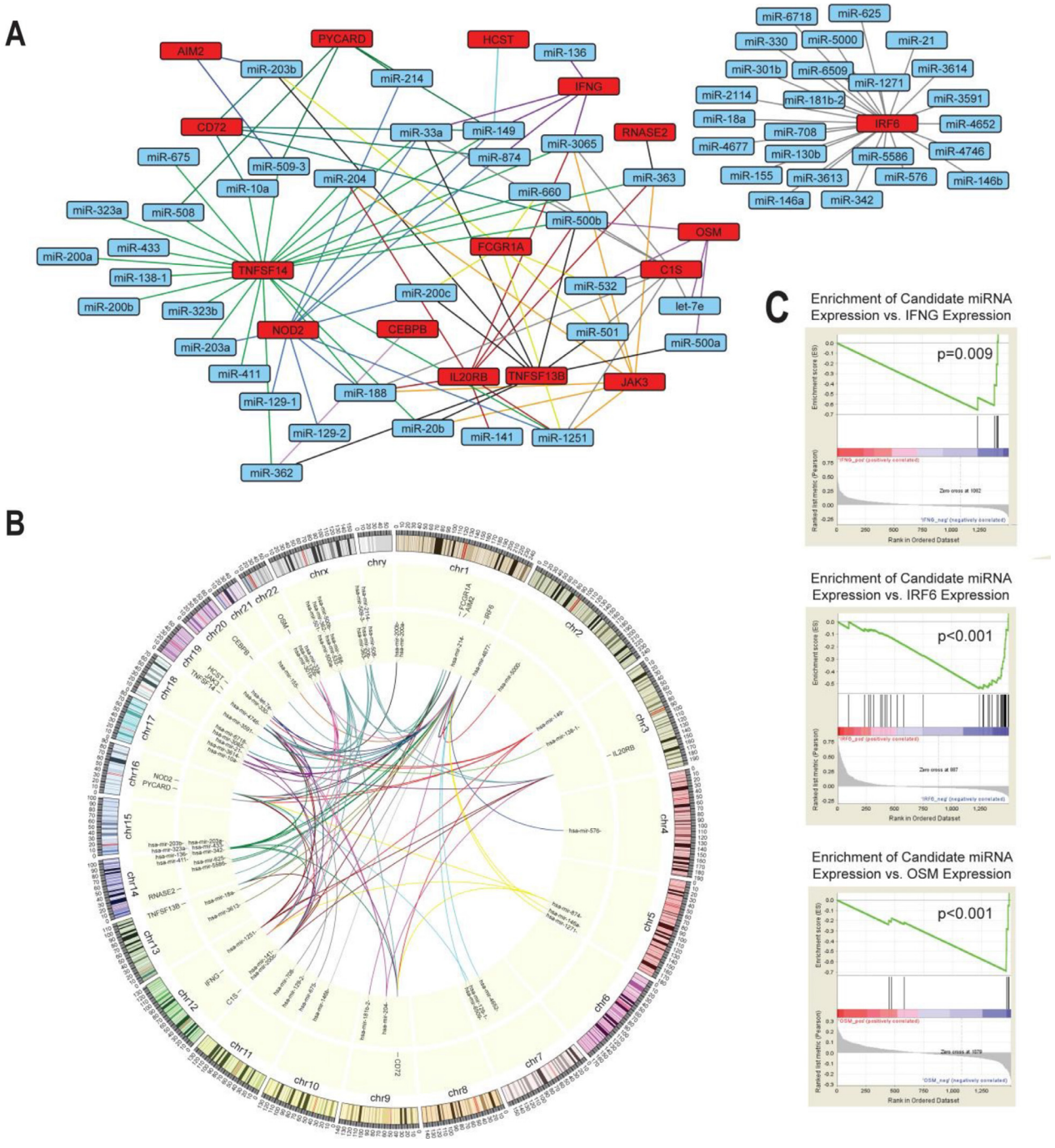

Fig. 4. Correlations between IA gene expression and regulatory miRNA expressions. (**A**) Plot of interactions between dysregulated IA genes and targeting miRNAs. (**B**) A Circos plot depicts the potential interactions between dysregulated miRNAs and dysregulated IA genes with their relative positions in the genome. Potential interactions are defined as interactions forming the leading edge subsets of each GSEA plot. (**C**) Sample gene set enrichment analysis plots indicate negative enrichment of miRNA expression in relation to expression of IA genes *IFNG*, *IRF6*, and *OSM*. All lines connecting to a single IA gene are of the same color in panels (A) and (B).

signal transduction or metabolism, which may be suggestive of tumor necrosis (Fig. 5F).

Discussion

To the best of our knowledge, we are the first to comprehensively profile dysregulation of immune-associated (IA) genes in ccRCC using whole transcriptome sequencing. We believe our evaluation of IA genes' modulation and clinical functionality in ccRCC may lend crucial insights into the reasons for differential patient response as well as suggest novel potential immunotherapeutic targets for further study. Using 512 ccRCC and 72 normal kidney RNA-seq datasets from TCGA, we identified a panel of 17 immune-associated (IA) genes most critical to the immune dysregulation landscape of ccRCC and most clinically actionable based on our collective correlation results, ranging from regulatory potential to clinical variable associations.

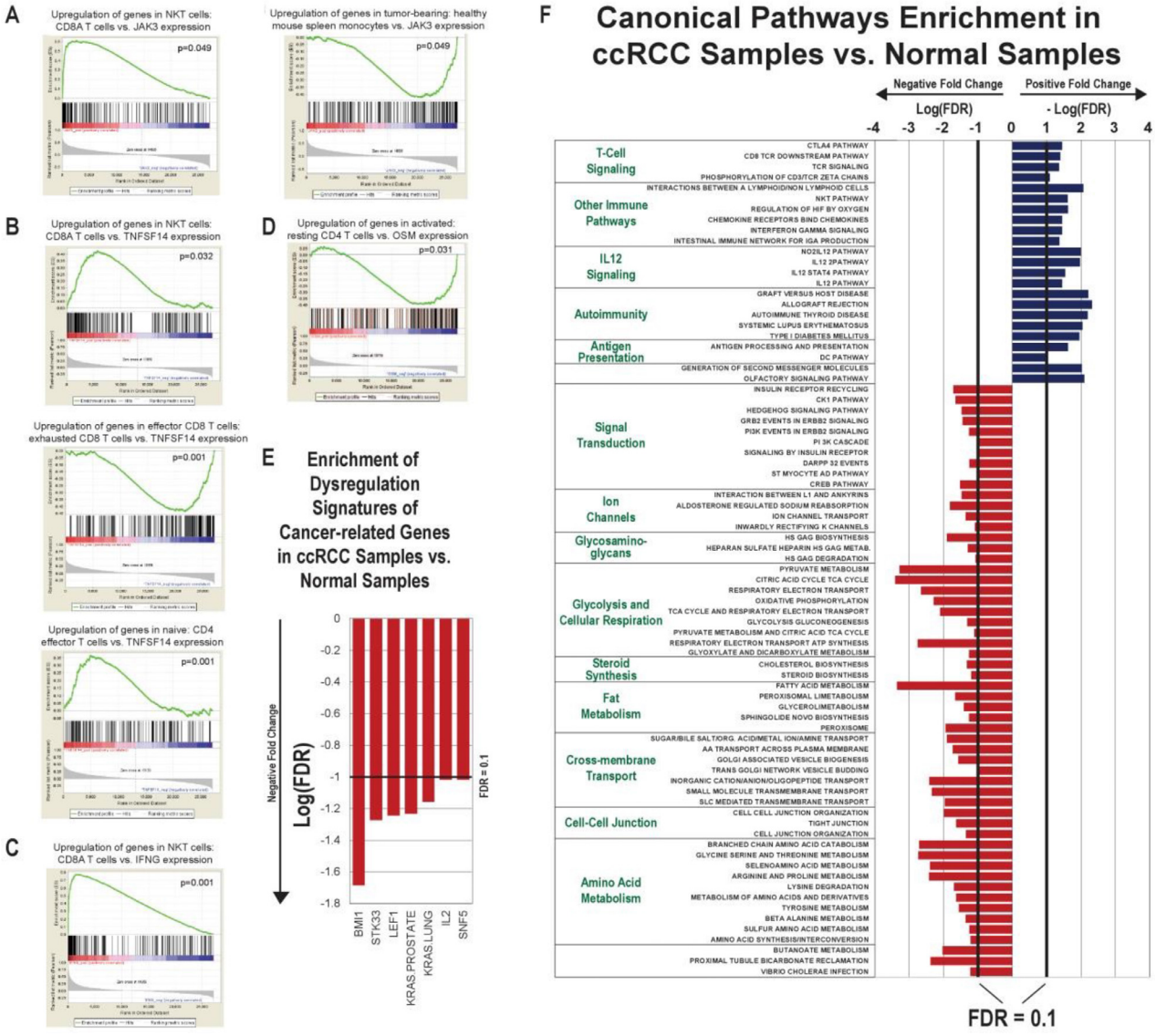

Fig. 5. Gene set-scale analysis of IA dysregulation. GSEA was used to associate the expression of (**A**) *JAK3*, (**B**) *TNFSF14*, (**C**) *IFNG*, and (**D**) *OSM* to expressions of genes in immunologic signatures ($p<0.05$). Bar graphs were plotted of GSEA enrichment result using fold change of gene expression in ccRCC vs. normal samples, against (**E**) cancer-related signatures and (**F**) canonical pathways as gene sets (FDR<0.1). Red bars indicate correlation with negative fold change for signatures of downregulated genes after knockdown of cancer-related genes in panel (**E**), while blue bars indicate correlation with negative fold change for signatures of downregulated genes after upregulation of cancer-related genes. Red bars indicate negative enrichment against fold change, and blue bars indicate positive enrichment against fold change in panel (F)

These 17 genes are involved in a wide variety of important immune processes. We found 4 genes, *JAK3, AIM2, PYCARD*, and *OSM*, that can potentially be involved in adaptive immune resistance. Adaptive immune resistance occurs when cancer cells are induced to evade the adaptive immune system in response to an active cytotoxic or inflammatory response [19]. In many cases, the cancer cell upregulates immune checkpoint receptors, such as PD-L1, when it is exposed to interferons or cytokines [19]. We found *JAK3*, a gene overactivated in various cancers and able to induce adaptive immune resistance, to be upregulated in ccRCCs [20,21]. Previous studies have shown that JAK3 may desensitize patients to PD-1 blockade by amplifying PD-1-related tumor cell preservation through PD-L1 overexpression [22]. We also identified *AIM2, PYCARD*, and *OSM*, three genes involved in the inflammatory response, to be upregulated in ccRCCs. AIM2 interacts with PYCARD (ASC) to activate caspase-1, which then cleaves and activates the pro-inflammatory cytokines IL-1b and IL-18 [23,24]. Caspase-1 activation is often the rate-limiting step in the pro-inflammatory response, thus *AIM2* and *PYCARD* may be useful targets in modulation of inflammation 24]. OSM, on the other hand, synergizes with TNF-a and IL-1b to enhance expression of the pro-inflammatory cytokine IL-6 in ccRCCs [25,26]. These proinflammatory cytokines have been documented to cause adaptive immune resistance through upregulation of PD-L1 [27,28].

Another IA gene, CMTM4, is recently found to increase PD-L1 levels by reducing ubiquitination of the PD-L1 protein at the cell surface, thereby increasing PD-L1 protein half-life [29]. However, we identified the IA gene *CMTM4* to be downregulated in ccRCCs. Although *CMTM4* downregulation seems to be inconsistent with oncogenesis in this context, *CMTM4* downregulation is in accordance with previous findings documenting tumor suppressive functions of *CMTM4* in ccRCC and is consistent with our correlation of higher *CMTM4* expression with increased patient survival. Therefore, we suspect that differences in the ratio of

expressions of CMTM4 and PD-L1-inducing genes may result in variable PD-L1 expressions for individual patients through their competing effects on PD-L1 regulation. *CMTM4* may also have alternate unknown functions that must be further investigated before it can be considered a therapeutic target for ccRCC.

2 of the 17 IA genes are also involved in NF-kB signaling, a pathway that has been found to regulate various aspects of RCC tumor biology that render conventional therapies ineffective, including resistance to apoptosis and multi-drug resistance [30]. We identified *TNFSF13B* and *TNFSF14*, both implicated in NF-kB activation, to be upregulated in ccRCC, suggesting that their inhibition may lead to improved patient outcomes [31]. However, TNFRSF13C, the receptor for TNFSF13B, is associated with higher likelihood of responding to PD-1 blockade according to our analysis of PD-1 blockade response signature. Therefore, *TNFSF13B*'s upregulation may actually contribute to ccRCC's ability to response to immunotherapy. On the other hand, *TNFSF14* has also been found to associate with improved patient survival in colon cancer due to its ability to drive cytotoxic T-cell response and enhance immune eradication of metastatic cancer cells, although this mechanism of action is not fully understood [32]. These NF-kB-associated TNF superfamily members should be further investigated clinically for their capacities of influencing immunotherapy response.

To identify possible intervention points to regulate the immune landscape of ccRCC, we identified key genomic alterations and miRNA regulators potentially associated with IA gene dysregulation. Notably, we found multiple IA genes to associate with deletion hotspots in chromosome arms 3p,14q, and 9p and an amplification hotspot in 20q. However, the genes within these regions that we found to correlate with IA genes dysregulation are not the same for each IA gene, suggesting that the event of genomic alteration, over specific genes the alterations target, may be more important to IA dysregulation. We found that several miRNAs, including miR-3065, miR-508, and miR-149, can potentially target a significant fraction of the 17 core IA genes, suggest that they may be valuable targets for ccRCC therapy. Specifically, miR-149, which may target PYCARD, IFNG, HCST, TNFSF14, CD72, and NOD2, has been found to be downregulated in various cancers, including ccRCC, and can suppress tumor formation and metastasis [33].

Our study implicates novel and attractive IA genes in ccRCC that should be further investigated for whether they can be used as targets for immunotherapy in ccRCC. Although much remains to be elucidated, we believe that our study sheds light on the relatively unexplored immune landscape of ccRCC to lay a foundation for future work on ccRCC immunotherapy.

Materials and methods

mRNA differential expression analyses

Level 3 normalized mRNA expression read counts for 512 ccRCC (KIRC) and 72 adjacent normal samples datasets were downloaded on 1 Sep 2017 from The Cancer Genome Atlas (TCGA) (https://tcga-data.nci.nih.gov/tcga). All samples collected for TCGA came from patients who have not received previous cancer treatments. mRNA read count tables (htseq files) were imported into edgeR v3.5 (http://www.bioconductor.org/packages/release/bioc/html/edgeR.html) as a DGE list. Lowly expressed mRNAs (counts-per-million < 1 in an amount of samples greater than the size of the smaller cohort of each analysis) were filtered from the analysis, and then TMM (trimmed mean of M-values) normalization factors, common dispersion, and tagwise dispersion were calculated for the expression matrix. Significantly differentially expressed mRNAs in ccRCC vs. normal samples were then identified using the exact test ($p < 0.05$). Immune-associated genes from which differentially expressed mRNAs were transcribed were identified as dysregulated and retained as candidates. Differential expression is defined as $p < 0.05$ and fold change < -2 or > 2 in edgeR analysis. All statistical tests performed in this study are two-tailed. A gene is determined to be immune-associated if it is related to any process in the innate or adaptive immune system based on existing literature.

Association of candidate genes' expressions with patient survival and clinical variables

Survival analyses were performed using the Kaplan-Meier Model, with gene expression designated as a binary variable based on expression above or below the median expression of all samples. Univariate Cox regression analysis was used to identify candidates significantly associated with patient survival ($p < 0.05$). Survival-correlated genes were evaluated for clinical significance. Employing the Kruskal-Wallis test, we investigated gene association with neoplasm histological grade, clinical and pathologic stages, vascular invasion of tumor, and percent lymphocyte infiltration using clinical data and mRNA expression values (counts-per-million) from ccRCC patients. In clinical T stage analysis, patients with stages T1a and T1b were grouped into stage T1, and likewise for stages T2, T3, and T4. Patients with no available information for a given variable were filtered from analyses involving that variable.

Results of clinical variable correlations are visualized with boxplots where all datapoints within the boxes are those in between the first and third quartiles, while the whiskers extend 1.5X the interquartile range (IQR) from the boundaries of the boxes, where IQR=quartile 3-quartile 1. Datapoints outside the whiskers are considered outliers. Datapoints outside 3X the IQR from the box boundaries are considered extreme outliers and are sometimes removed from the plot to improve visualization of the rest of the plots. No more than 5 points, out of 512 points, are removed in a given plot.

Information-coefficient based correlation of IA gene expression with genomic alterations

Mutation and SCNA data for the ccRCC tumors were obtained from mutation and SCNA annotation files generated by the Broad Institute GDAC Firehose on 28 January 2016. Annotation files were compiled into a binary input file for the program REVEALER (repeated evaluation of variables conditional entropy and redundancy), designed to computational identify a set of specific copy number alterations and mutations most likely responsible for the change in activity of a target profile. The target profile was defined in our study to be IA gene expression. In order to identify a set of most relevant genomic alterations, REVEALER runs multiple iterations of the correlation algorithm, with the genomic feature exhibiting the strongest correlation in each run serving as a seed for the successive run. We set the maximum number of iterations to three. A seed is a particular mutation or copy number gain or loss event that most likely accounts for the target activity. When given a seed, REVEALER will focus correlation on only patients with altered target activity not accounted for by the seed. Since we do not know which genomic alteration is responsible for the dysregulation of each gene, we set the seed for the first iteration to null. We set the threshold of genomic features to input to features present in less than 75% of all samples.

Identification of significant genes within each IA dysregulation-associated genomic locus

A complete list of genes located within each genomic cytoband was obtained using the Ensembl BioMart tool (https://www.ensembl.org/). Spearman correlation was then applied to correlate the expression of a dysregulated IA gene to the expressions of all genes within a cytoband whose amplification or deletion has been associated with the IA gene dysregulation by REVEALER ($p < 0.05$).

Assessing potential involvement of miRNAs in regulating IA genes

To identify possible regulatory miRNAs associated with IA genes, we identified a list of miRNAs predicted to bind to each dysregulated mRNA using TargetScan version 7.1 (http://www.targetscan.org/vert_71/) [34]. This list is then filtered to exclude any miRNAs not dysregulated in ccRCC. Dysregulation of miRNAs was determined by downloading miRNA expression datasets on 16 Sep 2017 of the same patients used earlier in mRNA differential expression analysis from TCGA, and identifying differential expression using edgeR as described earlier. Only miRNAs that were dysregulated in a direction consistent with their regulatory roles of IA genes (i.e. miRNAs that were upregulated if the IA gene was downregulated) were retained as candidates.

The GSEA software was used to characterize enrichment of miRNA expressions with respect to IA gene expressions. The full set of candidate miRNAs for each IA gene was modeled as a gene set. The continuous expression values of IA genes were used as phenotype labels. The unfiltered expression values of all miRNAs available from TCGA miRNA expression datasets were included in the expression dataset input file. One GSEA plot was produced for each IA gene potentially associated with seven or more candidate miRNAs.

Identification of immunologic signatures associated with IA gene expressions

Gene set signatures documenting differences in gene expression between different immunologic states (C7 gene set) were downloaded from MSigDB (http://software.broadinstitute.org/gsea/msigdb). 3492 relevant gene sets were filtered from the list of immunologic signatures downloaded and then analyzed for enrichment with respect to IA gene expressions using GSEA. Each gene set generally lists genes with the greatest change in expression following stimulation of specific immune cell types with different molecules, compared to a control sample. Other gene sets list genes with the greatest expression differences between two immune cell types or populations. With some exceptions, the top 200 genes with significant expression difference in a particular direction (decreased or elevated expression) are included in the gene set. The phenotype file for this analysis was identical to the GSEA performed for miRNA expression correlation. We replaced the expression dataset input file containing miRNA expression with one containing mRNA expression [35].

Identification of 17 key dysregulated IA genes

For all IA genes that are differentially expressed between ccRCC and normal samples, we performed survival correlation analyses to narrow the candidate list of important IA genes to over 300 survival-correlated dysregulated genes. The candidate IA genes' expressions were then correlated to clinical variables and immunologic signatures to determine the IA genes' clinical relevance and relevance to immune processes. The significance of differential expression analysis, survival correlations, clinical variable correlations, and immunologic signature correlations were all taken into account to establish a panel of 17 key IA genes in ccRCC by assigning each candidate gene a heuristic score. The score is described by the heuristic formula below:

if |differential expression fold change | > 2.05, +1 to score;
if univariate Cox regression p-value for survival correlation < 0.0015, +1 to score;
if sum of GSEA FDRs for immunologic signature correlations < 0.2, +1 to score;
if sum of Kruskal-Wallis p-values for clinical variable correlation > 0.074, +1 to score.

The score was used to further narrow the list of candidate genes, and the cutoff values used in the score were chosen to achieve approximately equal representation of the top genes from each of the 4 analyses and narrow the list of IA genes to less than 20.

Identification of dysregulated canonical pathways and oncogenic signature in ccRCC samples

GSEA was used to compute the enrichment of canonical pathways (C2: CP gene set, MSigDB) and oncogenic signatures (C6 gene set, MSigDB) in ccRCC samples vs. adjacent normal samples. The GSEA pre-ranked function was used for the enrichment, with all genes ranked by fold change of ccRCC vs. normal gene expressions. Although the recommended significance cutoff of enrichment is FDR=0.25, we filtered for significant pathways at FDR<0.1 for greater statistical power. The canonical pathways gene set includes a wide variety of biological processes and is not specific to cancer or immunology. The oncogenic signatures gene set lists genes downregulated or upregulated after a knockdown or overexpression of a cancer-related gene, which can be either a tumor suppressor or oncogene.

Conclusions

In this study, we explored the IA gene expression landscape in ccRCC and identified a panel of 17 key IA genes dysregulated in ccRCC. Within the 17 IA genes, several genes are involved in interleukin signaling, NF-kB signaling, and inflammation, respectively. We also identified key genomic alterations modulating the immune landscape in ccRCC and discovered that miRNAs may be key regulators of dysregulated IA genes. We believe the IA genes we identified may be potential targets for therapeutic intervention to improve current immunotherapy outcomes or to inform new immunotherapy strategies.

Declaration of Competing Interest

The authors declare no conflict of interest.

CRediT authorship contribution statement

Omar A. Saad: Validation, Formal analysis, Investigation, Writing – original draft, Visualization. **Wei Tse Li:** Methodology, Software, Validation, Formal analysis, Investigation, Writing – review & editing, Visualization. **Aswini R. Krishnan:** Validation, Investigation, Writing – original draft. **Griffith C. Nguyen:** Writing – review & editing. **Jay P. Lopez:** Writing – review & editing. **Rana R. McKay:** Writing – review & editing. **Jessica Wang-Rodriguez:** Resources, Writing – review & editing. **Weg M. Ongkeko:** Conceptualization, Methodology, Resources, Writing – review & editing, Supervision, Project administration, Funding acquisition.

Funding

This research was funded by the Academic Senate of the University of California San Diego, Grant No. RS167R-ONGKEKO.

Acknowledgments

Not applicable.

Supplementary materials

Supplementary material associated with this article can be found, in the online version, at doi:10.1016/j.neo.2021.12.007.

References

[1] Linehan WM. Genetic basis of kidney cancer: role of genomics for the development of disease-based therapeutics. *Genome Res* 2012;**22**:2089–100. doi:10.1101/gr.131110.111.

[2] Hutson TE. Renal cell carcinoma: diagnosis and treatment, 1994-2003. *Proc (Bayl Univ Med Cent)* 2005;**18**:337–40.

[3] Xing T, He H. Epigenomics of clear cell renal cell carcinoma: mechanisms and potential use in molecular pathology. *Chin J Cancer Res* 2016;**28**:80–91. doi:10.3978/j.issn.1000-9604.2016.02.09.

[4] Cowey CL, Rathmell WK. VHL gene mutations in renal cell carcinoma: role as a biomarker of disease outcome and drug efficacy. *Curr Oncol Rep* 2009;**11**:94–101.

[5] Rini BI. VEGF-targeted therapy in metastatic renal cell carcinoma. *Oncologist* 2005;**10**:191–7. doi:10.1634/theoncologist.10-3-191.

[6] Heidegger I, Pircher A, Pichler R. Targeting the tumor microenvironment in renal cell cancer biology and therapy. *Front Oncol* 2019;**9**:490. doi:10.3389/fonc.2019.00490.

[7] Chevrier S, Levine JH, Zanotelli VRT, Silina K, Schulz D, Bacac M, Ries CH, Ailles L, Jewett MAS, Moch H, et al. An Immune atlas of clear cell renal cell carcinoma. *Cell* 2017;**169**:736–49 e718. doi:10.1016/j.cell.2017.04.016.

[8] Giraldo NA, Becht E, Pages F, Skliris G, Verkarre V, Vano Y, Mejean A, Saint-Aubert N, Lacroix L, Natario I, et al. Orchestration and prognostic significance of immune checkpoints in the microenvironment of primary and metastatic renal cell cancer. *Clin Cancer Res* 2015;**21**:3031–40. doi:10.1158/1078-0432.CCR-14-2926.

[9] Sundar R, Cho BC, Brahmer JR, Soo RA. Nivolumab in NSCLC: latest evidence and clinical potential. *Ther Adv Med Oncol* 2015;**7**:85–96. doi:10.1177/1758834014567470.

[10] Motzer RJ, Escudier B, McDermott DF, George S, Hammers HJ, Srinivas S, Tykodi SS, Sosman JA, Procopio G, Plimack ER, et al. Nivolumab versus everolimus in advanced renal-cell carcinoma. *N Engl J Med* 2015;**373**:1803–13. doi:10.1056/NEJMoa1510665.

[11] Kammerer-Jacquet SF, Deleuze A, Saout J, Mathieu R, Laguerre B, Verhoest G, Dugay F, Belaud-Rotureau MA, Bensalah K, Rioux-Leclercq N. Targeting the PD-1/PD-L1 pathway in renal cell carcinoma. *Int J Mol Sci* 2019;**20**. doi:10.3390/ijms20071692.

[12] McDermott DF, Huseni MA, Atkins MB, Motzer RJ, Rini BI, Escudier B, Fong L, Joseph RW, Pal SK, Reeves JA, et al. Clinical activity and molecular correlates of response to atezolizumab alone or in combination with bevacizumab versus sunitinib in renal cell carcinoma. *Nat Med* 2018;**24**:749–57. doi:10.1038/s41591-018-0053-3.

[13] Miao D, Margolis CA, Gao W, Voss MH, Li W, Martini DJ, Norton C, Bossé D, Wankowicz SM, Cullen D, et al. Genomic correlates of response to immune checkpoint therapies in clear cell renal cell carcinoma. *Science* 2018;**359**:801–6. doi:10.1126/science.aan5951.

[14] Mennitto A, Grassi P, Ratta R, Verzoni E, Prisciandaro M, Procopio G. Nivolumab in the treatment of advanced renal cell carcinoma: clinical trial evidence and experience. *Ther Adv Urol* 2016;**8**:319–26. doi:10.1177/1756287216656811.

[15] Melton C, Reuter JA, Spacek DV, Snyder M. Recurrent somatic mutations in regulatory regions of human cancer genomes. *Nat Genet* 2015;**47**:710–16. doi:10.1038/ng.3332.

[16] Beroukhim R, Mermel CH, Porter D, Wei G, Raychaudhuri S, Donovan J, Barretina J, Boehm JS, Dobson J, Urashima M, et al. The landscape of somatic copy-number alteration across human cancers. *Nature* 2010;**463**:899–905. doi:10.1038/nature08822.

[17] Kim JW, Botvinnik OB, Abudayyeh O, Birger C, Rosenbluh J, Shrestha Y, Abazeed ME, Hammerman PS, DiCara D, Konieczkowski DJ, et al. Characterizing genomic alterations in cancer by complementary functional associations. *Nat Biotechnol* 2016;**34**:539–46. doi:10.1038/nbt.3527.

[18] Nair S, Dhodapkar MV. Natural killer T cells in cancer immunotherapy. *Front Immunol* 2017;**8**:1178. doi:10.3389/fimmu.2017.01178.

[19] Ribas A. Adaptive immune resistance: how cancer protects from immune attack. *Cancer Discov* 2015;**5**:915–19. doi:10.1158/2159-8290.CD-15-0563.

[20] Li SD, Ma M, Li H, Waluszko A, Sidorenko T, Schadt EE, Zhang DY, Chen R, Ye F. Cancer gene profiling in non-small cell lung cancers reveals activating mutations in JAK2 and JAK3 with therapeutic implications. *Genome Med* 2017;**9**:89. doi:10.1186/s13073-017-0478-1.

[21] Behbahani TE, Thierse C, Baumann C, Holl D, Bastian PJ, von Ruecker A, Muller SC, Ellinger J, Hauser S. Tyrosine kinase expression profile in clear cell renal cell carcinoma. *World J Urol* 2012;**30**:559–65. doi:10.1007/s00345-011-0767-z.

[22] Maleki Vareki S, Garrigos C, Duran I. Biomarkers of response to PD-1/PD-L1 inhibition. *Crit Rev Oncol Hematol* 2017;**116**:116–24. doi:10.1016/j.critrevonc.2017.06.001.

[23] Fernandes-Alnemri T, Yu JW, Datta P, Wu J, Alnemri ES. AIM2 activates the inflammasome and cell death in response to cytoplasmic DNA. *Nature* 2009;**458**:509–13. doi:10.1038/nature07710.

[24] Franchi L, Eigenbrod T, Munoz-Planillo R, Nunez G. The inflammasome: a caspase-1-activation platform that regulates immune responses and disease pathogenesis. *Nat Immunol* 2009;**10**:241–7. doi:10.1038/ni.1703.

[25] Van Wagoner NJ, Choi C, Repovic P, Benveniste EN. Oncostatin M regulation of interleukin-6 expression in astrocytes: biphasic regulation involving the mitogen-activated protein kinases ERK1/2 and p38. *J Neurochem* 2000;**75**:563–75.

[26] Palmqvist P, Lundberg P, Lundgren I, Hanstrom L, Lerner UH. IL-1beta and TNF-alpha regulate IL-6-type cytokines in gingival fibroblasts. *J Dent Res* 2008;**87**:558–63. doi:10.1177/154405910808700614.

[27] Kaplanov I, Carmi Y, Kornetsky R, Shemesh A, Shurin GV, Shurin MR, Dinarello CA, Voronov E, Apte RN. Blocking IL-1beta reverses the immunosuppression in mouse breast cancer and synergizes with anti-PD-1 for tumor abrogation. *Proc Natl Acad Sci U S A* 2019;**116**:1361–9. doi:10.1073/pnas.1812266115.

[28] Lamano JB, Lamano JB, Li YD, DiDomenico JD, Choy W, Veliceasa D, Oyon DE, Fakurnejad S, Ampie L, Kesavabhotla K, et al. Glioblastoma-derived IL6 induces immunosuppressive peripheral myeloid Cell PD-L1 and promotes tumor growth. *Clin Cancer Res* 2019;**25**:3643–57. doi:10.1158/1078-0432.CCR-18-2402.

[29] Mezzadra R, Sun C, Jae LT, Gomez-Eerland R, de Vries E, Wu W, Logtenberg MEW, Slagter M, Rozeman EA, Hofland I, et al. Identification of CMTM6 and CMTM4 as PD-L1 protein regulators. *Nature* 2017;**549**:106–10. doi:10.1038/nature23669.

[30] O'Leary T, Wyllie DJ. The ups and downs of synaptic plasticity: influences on this particular 'market. *J Physiol* 2008;**586**:5839–40. doi:10.1113/jphysiol.2008.165720.

[31] Heo SK, Noh EK, Gwon GD, Kim JY, Jo JC, Choi Y, Koh S, Baek JH, Min YJ, Kim H. LIGHT (TNFSF14) increases the survival and proliferation of human bone marrow-derived mesenchymal stem cells. *PLoS One* 2016;**11**:e0166589. doi:10.1371/journal.pone.0166589.

[32] Qin JZ, Upadhyay V, Prabhakar B, Maker AV. Shedding LIGHT (TNFSF14) on the tumor microenvironment of colorectal cancer liver metastases. *J Transl Med* 2013;**11**:70. doi:10.1186/1479-5876-11-70.

[33] Okato A, Arai T, Yamada Y, Sugawara S, Koshizuka K, Fujimura L, Kurozumi A, Kato M, Kojima S, Naya Y, et al. Dual strands of pre-miR-149 inhibit cancer cell migration and invasion through targeting FOXM1 in renal cell carcinoma. *Int J Mol Sci* 2017;**18**. doi:10.3390/ijms18091969.

[34] Agarwal V, Bell GW, Nam J-W, Bartel DP, Ameres SL, Martinez J, Schroeder R, Anders G, Mackowiak SD, Jens M, et al. Predicting effective microRNA target sites in mammalian mRNAs. *eLife* 2015;**4**:101–12. doi:10.7554/eLife.05005.

[35] Subramanian A, Tamayo P, Mootha VK, Mukherjee S, Ebert BL, Gillette MA, Paulovich A, Pomeroy SL, Golub TR, Lander ES, et al. Gene set enrichment analysis: a knowledge-based approach for interpreting genome-wide expression profiles. *Proc Natl Acad Sci U S A* 2005;**102**:15545–50. doi:10.1073/pnas.0506580102.